

Investigation of Protonation Efficiency for Amino Acids in Matrix-Assisted Laser Desorption/Ionization

Masashi Tsuge and Kennosuke Hoshina*

Department of Pharmacy, Niigata University of Pharmacy and Applied Life Sciences, 265-1 Higashijima, Akiha-ku, Niigata 956-8603

Received March 18, 2010; E-mail: hoshina@nupals.ac.jp

MALDI spectra for 20 natural amino acids were measured at various mixing ratios of amino acid (A) and matrix (M: CHCA or DHB) to clarify the main protonation process as well as MALDI plume conditions, which affect the detection sensitivity of analytes in MALDI. Signal intensities of protonated amino acids (AH^+) relative to protonated matrix (MH^+), obtained as AH^+/MH^+, revealed a clear correlation between AH^+/MH^+ and the gas-phase basicity (GB) of the respective amino acids except for three basic amino acids, Lys, His, and Arg. This relationship between AH^+/MH^+ and GB was interpreted in terms of a protonation model in which AH^+ is produced through a reversible proton-transfer reaction of $MH^+ + A \rightleftharpoons M + AH^+$ reaching thermal equilibrium in the MALDI plume. The GB of matrix molecules and MALDI plume temperatures independently determined from analysis of the present data (851 kJ mol^{-1} and 1510 K for CHCA and 830 kJ mol^{-1} and 1330 K for DHB) agreed well with values in the literature, indicating the validity of the present interpretation. The ratios AH^+/MH^+ for Lys, His, and Arg had lower values than those expected from the GB by a factor of 10^{-1}–10^{-2}. This discrepancy could have been caused by proton acceptance by amino groups in amino acids, which are caused by an intramolecular hydrogen bond, determine the magnitude of the GB for basic amino acids.

Matrix-assisted laser desorption/ionization mass spectrometry (MALDI-MS) is widely used as a soft ionization method for thermally labile samples like biomolecules.[1,2] High sensitivity on the order of subfemtomoles,[3] corresponding to the lower limit required for detection, has been achieved by trial and error through developments in matrix reagents, sample preparation protocols, laser desorption conditions, and so on. Despite such developments, the elemental processes involved in the protonation of analytes have not been intensively investigated. For further improvement in the sensitivity of MALDI measurement, the processes affecting protonation efficiency must be identified.

Ion formation in MALDI reportedly involves three processes, which are:[4] (1) heating of matrix molecules to 400–1100 K by the absorption of laser irradiation and subsequent sublimation of an analyte (A)/matrix (M) mixture to form a MALDI plume; (2) ionization of matrix molecules in the MALDI sample or plume,[5,6] called the primary ion formation process, in which radical cations (M^+) and protonated matrix (MH^+) are formed as key species for the third process; and (3) ionization of the analyte, called the secondary ion formation process, to form three types of positive ions, cationized ions (ANa^+ and AK^+), radical cations ($A^{+\bullet}$), and protonated ions (AH^+). Among these ions produced in secondary ion formation, the ion signal of AH^+ is the principal peak of the analyte in MALDI-MS spectra and is commonly used for the detection of analytes. The protonated analyte ion is thought to be formed by the reaction

$$MH^+ + A \rightleftharpoons M + AH^+ \quad (1)$$

where a proton is transferred from protonated matrix MH^+ to the analyte, forming protonated analyte AH^+. If the reaction reaches thermal equilibrium in a dense, hot MALDI plume, the amount of AH^+ should depend on the value of the gas-phase basicity (GB) of the analyte GB(A) relative to that of the matrix GB(M).[7] In other words, the protonation efficiency of the analyte is expected to increase as GB(A) increases when using the same matrix reagent.

Kinsel et al.[8] verified this model by measuring MALDI spectra of amino acids (Gly, Ala, Val, Ile, and Phe)/α-cyano-4-hydroxycinnamic acid (CHCA) matrix samples; they found that the yield of AH^+ relative to ($MH^+ + M^+$) increased as the GB of the amino acid increased. This correlation was interpreted in terms of a thermochemical treatment in which the equilibrium conditions of reaction (1) were achieved in the MALDI plume. Nishikaze and Takayama[9] reported a similar correlation between ion yields of AH^+ and proton affinity for 20 natural amino acids, although Lys deviated greatly from the correlation.

In the present study, we measured MALDI-MS spectra for 20 natural amino acids using two different matrix reagents, CHCA and 2,5-dihydroxybenzoic acid (DHB), at various A/M mixing ratios in the range of 1×10^{-5} to 10. Based on the intensity ratios of AH^+/MH^+ derived from secure analyses of more than 9000 MALDI spectra, we demonstrated that the relationship between protonation efficiency and GB is interpreted accurately by assuming thermal equilibrium in reaction (1), except for basic amino acids. Based on the results of these analyses, the differences in protonation efficiency between CHCA and DHB and deviations from the correlation for the basic amino acids are also discussed to confirm the validity of the protonation model.

Published on the web October 5, 2010; doi:10.1246/bcsj.20100080

Experimental

Materials. MALDI matrices, CHCA and DHB, and 17 amino acids (Ala, Arg, Asn, Asp, Cys, Gln, Glu, Gly, His, Ile, Leu, Lys, Met, Pro, Ser, Thr, and Val) were purchased from Wako Pure Chemicals. Trp, Tyr, and Phe were purchased from Sigma Aldrich. The solvents (ultrapure water, acetonitrile, and trifluoroacetic acid) were also purchased from Wako Pure Chemicals.

Sample Preparation. MALDI samples were prepared by a common dried-droplet method.[10] In brief, 1 μL of amino acid aqueous solution (typically ranging from 0.5 nmol mL^{-1} to 500 μmol mL^{-1}) and 1 μL of DHB matrix solution (50 μmol mL^{-1} in water) or CHCA matrix solution (50 μmol mL^{-1} in 1:1 v/v water/acetonitrile with 0.1% trifluoroacetic acid) were deposited on a ground steel target plate. The mixtures were evaporated in air at room temperature. More than three MALDI samples for each of the 20 analyte/matrix ratios in the range of 1×10^{-5} to 10 were prepared to increase the accuracy of the MALDI signals.

MALDI-MS Measurement. Positive-ion mass spectra were measured using a MALDI time-of-flight (TOF) spectrometer (Autoflex III, Bruker Daltonics, Germany). Measurements were performed in the reflectron mode at an acceleration voltage of 19 kV, and each spectrum was obtained by accumulating 2000 laser shots (355 nm, <100 μJ/pulse, 200 Hz). The laser irradiating positions were displaced randomly on the MALDI sample every 10 shots to minimise fluctuation of the signal intensity as a result of non-uniform crystallization. Five spectra were measured for each of three MALDI samples with the same sample/matrix ratio, and thus a total of 15 spectra were obtained for each condition. Thus, ion yields were securely derived from the analyses of 15 spectra with a standard error.

Theoretical Model for Protonation Efficiency in MALDI

When proton transfer (1) in the MALDI plume reaches thermal equilibrium, the equilibrium constant, defined by $([M][AH^+])/([MH^+][A])$, and the change in Gibbs energy of reaction (1) at the standard condition ΔG° are related by

$$\Delta G^\circ = -RT \ln \frac{[M][AH^+]}{[MH^+][A]} \tag{2}$$

In the MALDI plume, the fraction of protonated molecules is estimated to be about 10^{-5}–10^{-3} of desorbed molecules,[11,12] i.e., $[M] \gg [MH^+]$ and $[A] \gg [AH^+]$. The ratio [A]/[M] in the MALDI plume can thus be approximated by the analyte/matrix ratio $([A]/[M])^0$, which stands for the mixing ratio applied to the sample plate,

$$\left(\frac{[A]}{[M]}\right)^0 \approx \frac{[A]+[AH^+]}{[M]+[MH^+]} \approx \frac{[A]}{[M]} \tag{3}$$

By substituting eq 3 into eq 2, we obtain the relation

$$\ln\left(\frac{[A]}{[M]}\right)^0_e = \frac{\Delta G^\circ}{RT} \tag{4}$$

where $([A]/[M])^0_e$ is defined as the analyte/matrix mixing ratio that provides $[MH^+] = [AH^+]$ in the MALDI plume; i.e., the resultant MH^+ and AH^+ signals are observed with the same intensities in the mass spectra. The ΔG° of reaction (2) corresponds to a difference in the GB of the analyte and matrix,

$$\Delta G^\circ = \mathrm{GB(M)} - \mathrm{GB(A)} \tag{5}$$

Consequently, we obtain the following equation:

$$\ln\left(\frac{[A]}{[M]}\right)^0_e = -\frac{\mathrm{GB(A)}}{RT} + \frac{\mathrm{GB(M)}}{RT} \tag{6}$$

Equation 6 implies that a log–log plot of experimentally determined $([A]/[M])^0_e$ with respect to GB(A) reveals a linear relationship with a slope of $-1/RT$ and an intersection of $\mathrm{GB(M)}/RT$ if the protonation of the analyte is completed through reaction (1) under thermal equilibrium.

Results and Discussion

MALDI-MS Spectra. Figure 1 shows typical MALDI-MS spectra measured for Arg/CHCA at three amino acid/matrix mixing ratios, $([A]/[M])^0 = 1$, 10^{-4}, and 10^{-6}, where [M] was fixed to be 50 μmol mL^{-1}. As shown in Figure 1a, at a higher mixing ratio, $([A]/[M])^0 = 1$, the strong signal of the protonated Arg ($Arg{\cdot}H^+$) at $m/z = 175$ is observed while signals originating from CHCA are suppressed due to the proton transfer in eq 1. As the fraction of amino acid decreases, the intensities of protonated CHCA matrix ($CHCA{\cdot}H^+$) at $m/z = 190$, $(CHCA–H_2O){\cdot}H^+$ at $m/z = 172$, and radical cation ($CHCA^{+\bullet}$) at $m/z = 189$ increase. At the mixing ratio of $([A]/[M])^0 = 10^{-6}$ shown in Figure 1c, the intensity of the $Arg{\cdot}H^+$ signal decreases to 0.01 of $CHCA{\cdot}H^+$. This alternation between signal intensities of AH^+ and MH^+ were

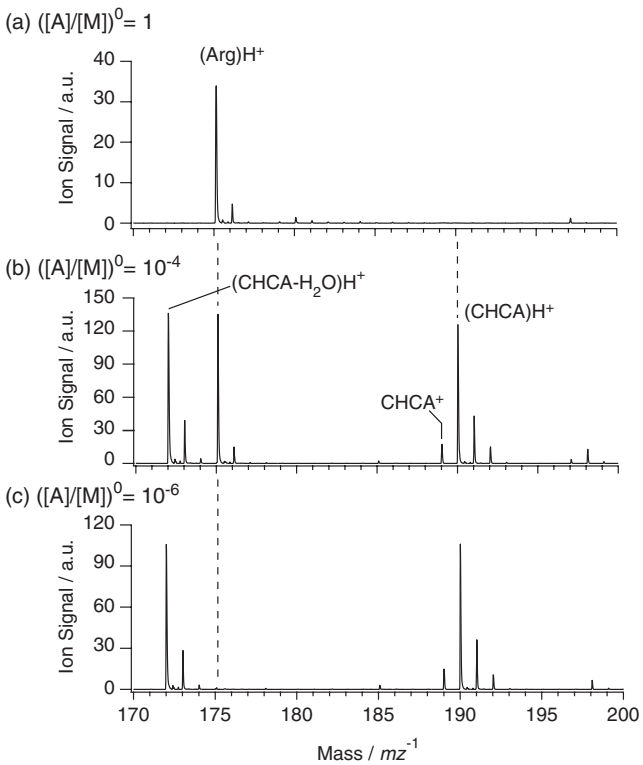

Figure 1. MALDI-MS spectra of Arg/CHCA measured at mixing ratios of $([A]/[M])^0 = 1$ (a), 10^{-4} (b), and 10^{-6} (c). Satellite peaks at $m/z = 173$, 176, 191, and 192 are assigned to ^{13}C or ^{15}N isotopomers.

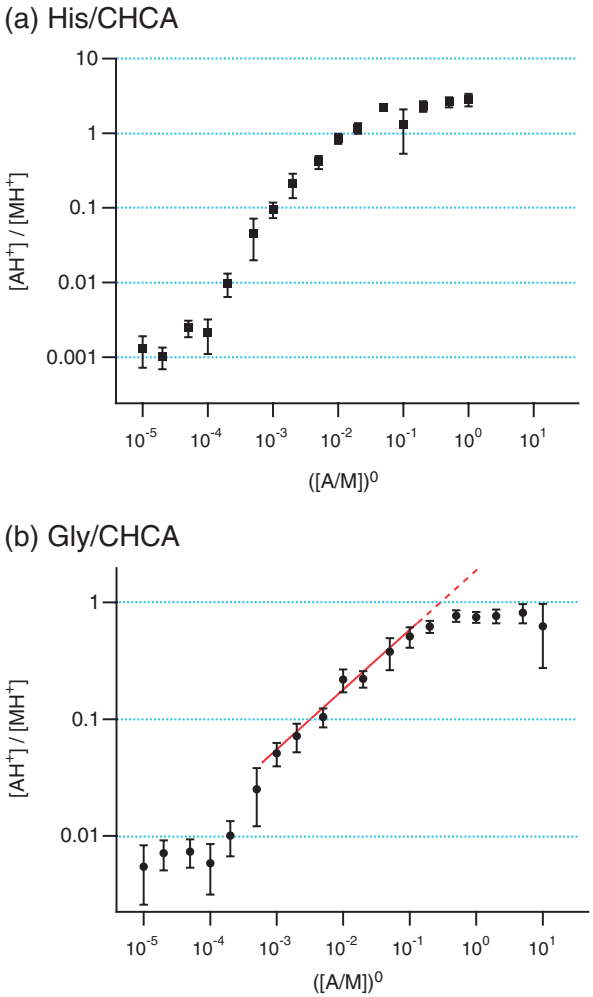

Figure 2. Logarithmic plots of $[AH^+]/[MH^+]$ versus A/M mixing ratio $([A]/[M])^0$ for (a) His/CHCA and (b) Gly/CHCA systems. Both plots exhibit a linear increase that becomes a plateau at lower and higher $([A]/[M])^0$. Solid line in (b) is the result of least-squares fitting for the linear region between 10^{-5} and 10^{-1}. Dashed line represents an extrapolation of the linear region to determine the value of $([A]/[M])^0_e$.

observed in common for all amino acids/matrix samples examined in this study.

Plot of $[AH^+]/[MH^+]$ as a Function of Analyte/Matrix Ratio. MALDI-MS spectra were measured at 20 analyte/matrix ratios $([A]/[M])^0$ typically ranging from 1×10^{-5} to 10 for each amino acid. From analyses of the measured spectra, the yield of the protonated amino acid relative to the protonated matrix, $[AH^+]/[MH^+]$, were derived. Figures 2a and 2b show logarithmic plots of $[AH^+]/[MH^+]$ observed in MALDI-MS spectra as a function of analyte/matrix ratio for Gly/CHCA and His/CHCA systems, respectively. Both plots have a plateau region at $([A]/[M])^0 \leq 10^{-4}$, begin to increase linearly at $([A]/[M])^0 = 10^{-4}$ and plateau again at $([A]/[M])^0 \geq 4 \times 10^{-1}$ for Gly/CHCA and at $([A]/[M])^0 \geq 6 \times 10^{-2}$ for His/CHCA. This characteristic (plateau–linear increase–plateau) was common in the plots for other amino acid/CHCA systems that we examined. The linear increase can be explained by the equation

$$\ln \frac{[AH^+]}{[MH^+]} = \ln \left(\frac{[A]}{[M]} \right)^0 - \frac{\Delta G^\circ}{RT} \quad (7)$$

derived from eqs 2 and 3. Equation 7 implies that the log–log plots shown in Figures 2a and 2b have a slope of one. Indeed, the slope of the linear regions was nearly one in all the systems, indicating that reaction (1) reached thermal equilibrium at the region $([A]/[M])^0$. The plateau at the higher $([A]/[M])^0$ is thought to be a result of the matrix suppression effect,[13,14] and there is no clear explanation for that at lower $([A]/[M])^0$. Both plateau behaviors suggest that AH^+ was formed by reaction (1) under nonequilibrium conditions, or the approximation in eq 3 does not hold good at these $([A]/[M])^0$ regions for CHCA. In the case of DHB, the plots do not exhibit plateaus in the $([A]/[M])^0$ range 10^{-5}–10. The difference in behavior between DHB and CHCA has been reported and was investigated by the usual dried droplet, and was attributed to poor cocrystallization in DHB.[13]

Determination of $([A]/[M])^0_e$ Values. The sample/matrix ratios $([A]/[M])^0_e$ at which AH^+ and MH^+ signals were observed with the same intensity, i.e., $[AH^+]/[MH^+] = 1$, were determined from the log–log plots of $[AH^+]/[MH^+]$ against $([A]/[M])^0$ in Figures 2a and 2b. In the case of the His/CHCA system in Figure 2a, $([A]/[M])^0_e$ was determined to be 1.42×10^{-2}. In contrast, as seen in Figure 2b, the $[AH^+]/[MH^+]$ plot for the Gly/CHCA system shows a plateau below $[AH^+]/[MH^+] = 1$ as a result of the matrix suppression effect. This means that in the Gly/CHCA system, this $([A]/[M])^0$ region deviates from the equilibrium assumption expressed by eq 7. Similar behaviors were observed in the Asp/CHCA, Glu/CHCA, and Tyr/CHCA systems. For these systems, $([A]/[M])^0_e$ values were determined by extrapolating the linear increase region, which conforms to eq 7, as demonstrated in Figure 2b, and $([A]/[M])^0_e = 0.42$ was obtained for the Gly/CHCA system. The $([A]/[M])^0_e$ values determined for the 20 amino acids are summarized in Table 1 along with the corresponding GB values.[15]

Gas-Phase Basicity of Matrices and Temperature of the MALDI Plume. Figure 3 shows $([A]/[M])^0_e$ values for 20 amino acids obtained using CHCA and DHB as matrices with respect to the GB of the amino acids. The plots exhibit linear relations with negative slopes for both CHCA and DHB matrices, indicating that the results can be analyzed in accordance with eq 6. The data of Lys, which belongs to basic amino acids, seem to be deviated largely from the trend. Similar exceptional behavior of Lys in the protonation efficiency was previously reported.[9] When least-squares fits were performed excluding the basic amino acids, Lys, His, and Arg, the data were fitted with a correlation coefficient of 0.76 for DHB while the three amino acids were out of the 95% confidence interval, estimated from a standard deviation of the fit. Similarly, data obtained for CHCA was also fitted with a correlation coefficient of 0.78 excluding the data of the three basic amino acids. The lines drawn in Figure 3 represent the results of the least-squares fits to eq 6. The values of the basic amino acids are one or two orders of magnitude larger than those expected from their GB(A) shown by the dashed lines in Figure 3.

The values of amino acids except for the basic amino acids were within one order of the predicted values, 0.3(Leu)–

3.8(Thr) for CHCA and 0.1(Asp)–5.4(Phe) for DHB. These factors correspond to the desorption efficiency of amino acid relative to matrix assuming that the fit residuals are attributed to a difference in the desorption efficiency. This means that the desorption efficiency is 0.3 times smaller than CHCA for Leu/CHCA sample, for instance.

Table 1. Gas-Phase Basicity (GB) and $([A]/[M])_e^0$ Values Measured for 20 Amino Acids Using CHCA and DHB Matrices

	Gas-phase basicity[a] /kJ mol^{-1}	$([A]/[M])_e^{0}$ [b]	
		CHCA	DHB
Gly	852.2	4.2×10^{-1} [c]	9.7×10^{-2}
Ala	867.7	3.8×10^{-1}	2.9×10^{-2}
Cys	869.3	5.7×10^{-1}	7.4×10^{-3}
Asp	872.8	3.5×10^{-1} [c]	1.6×10^{-1}
Val	876.7	2.2×10^{-1}	2.4×10^{-2}
Glu	879.1	3.9×10^{-2} [c]	4.2×10^{-3}
Leu	880.6	3.2×10^{-1}	3.2×10^{-2}
Ser	880.7	8.6×10^{-2}	2.5×10^{-2}
Ile	883.5	4.1×10^{-2}	1.0×10^{-2}
Thr	885.8	1.8×10^{-2}	1.5×10^{-2}
Pro	886.0	2.2×10^{-2}	2.8×10^{-3}
Phe	888.9	8.1×10^{-2}	9.3×10^{-4}
Asn	890.4	4.4×10^{-2}	1.3×10^{-2}
Tyr	891.6	1.8×10^{-2} [c]	1.2×10^{-3}
Met	901.5	2.8×10^{-2}	2.8×10^{-3}
Gln	902.1	2.5×10^{-2}	7.2×10^{-4}
Trp	915.0	2.4×10^{-2}	6.2×10^{-4}
His	950.2	1.4×10^{-2}	4.5×10^{-4}
Lys	951.0	4.9×10^{-2}	5.1×10^{-3}
Arg	991.6	2.1×10^{-4}	1.5×10^{-5}

a) Evaluated values from Ref. 15. b) Defined as the sample mixing ratio at which AH^+ and MH^+ were observed with the same intensity (see text). c) Determined by extrapolation (see text).

From the slopes and intersections of the fitting functions, GB(M) and plume temperature (T_p) can be determined. GB(M) = 851 kJ mol^{-1} and T_p = 1510 K for CHCA and GB(M) = 830 kJ mol^{-1} and T_p = 1330 K for DHB were obtained as optimised values; they are listed in Table 2 with values from the literature. The GB value of DHB obtained in the present work agrees well with the literature values of 822.5 ± 15.5,[16] 822 ± 8,[17] and 819.8 kJ mol^{-1}.[18] The GB value for CHCA determined in this work is between two literature values, 826.2 kJ mol^{-1} (Kinsel et al.[8]) and 900.5 ± 8.5 kJ mol^{-1}, which was determined using reaction bracketing by Steenvoorden et al.[16] These results validated the analysis using the protonation model in which proton transfer (1) between the matrix and amino acids reaches thermal equilibrium.

The estimated temperature for CHCA is close to the value T_p(CHCA) = 1730 K reported by Kinsel et al. using a method

Table 2. Gas-Phase Basicity/kJ mol^{-1} of CHCA and DHB Matrices

	CHCA	DHB
This work	851	830
Steenvoorden et al.[a]	900.5 ± 8.5	822.5 ± 15.5
Kinsel et al.[b]	826.2	—
Mormann et al.[c]	—	822 ± 8
Yassin and Marynick[d]	—	819.8

a) Measured by reaction bracketing (Ref. 16). b) Calculated at the B3LYP/6-311+G(2df,p)//B3LYP/6-31G(d,p) level of theory (Ref. 8). c) Measured thermokinetically (Ref. 17). d) Calculated at the B3LYP/6-311++G(2df,p)//B3LYP/6-31+G(d,p) level of theory (Ref. 18).

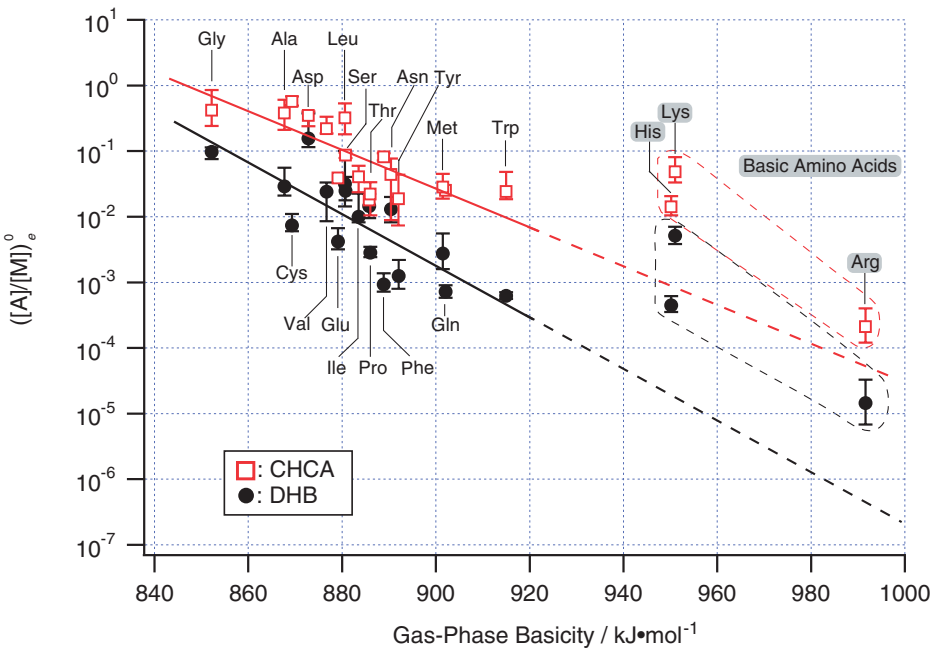

Figure 3. Logarithmic plot of $([A]/[M])_e^0$ as a function of the GB of amino acids obtained using CHCA (open squares) and DHB (filled circles) as matrix reagents. Solid lines were derived from a least squares fitting to eq 6, from which the basic amino acids His, Lys, and Arg were excluded for both plots.

similar to the one used in this study.[8] However, it is higher than the values (400–1100 K) determined as plume temperatures through different methods like measurement of internal energies of desorbed neutrals[19] and detection of blackbody radiation emitted from the sample surface.[20] This difference in T_p suggests that AH^+ formation proceeds in the high-temperature spatio-temporal region in the MALDI plume.

Low Protonation Efficiency in Basic Amino Acids in MALDI. As demonstrated clearly in Figure 3, basic amino acids Lys, His, and Arg revealed low protonation efficiencies compared to those expected from their GBs by a factor of 10^{-1} to 10^{-2}. These characteristic behaviors of the basic amino acids are believed to originate from a difference in the molecular site that functions as a proton acceptor. GB values were measured as a property of proton affinity for amino acids having canonical forms in the gas phase, in which the amino group acts as a proton acceptor, whereas side chains perform this role for basic amino acids.[15]

Judging from the results obtained in this study for amino acids with small GB, it can be said that an amino acid desorbed as a canonical form in the MALDI plume accepts a proton from MH^+ by its amino group to form AH^+, although they have a zwitterionic form in crystals. This is due to instability of the zwitterions; for example, the zwitterion of Gly is ca. 90 kJ mol^{-1} higher in energy than the canonical form. When Gly is isolated as a zwitterion, it assumes the canonical form immediately through non-barrier proton rearrangement from amino group to carbonyl group.[21]

In the case of basic amino acids, the difference in energy between zwitterionic and canonical forms decreases (for example, it is 15 kJ mol^{-1} for Arg), and they may be desorbed as zwitterions by retaining their structure in the sample/matrix mixture. According to a theoretical prediction, the zwitterion of Arg has a ring structure because of an intramolecular hydrogen bond between NH^+ in the guanidine side chain and the COO^- group.[22] This hydrogen bond prevents proton acceptance by the side chain, resulting in lower protonation efficiency because of proton acceptance by the amino group with a lower proton affinity.

Conclusion

MALDI-MS spectra of 20 amino acids were systematically measured using two different matrices, CHCA and DHB, at various analyte/matrix ratios in the range of 10^{-5} to 10. The ratios $[AH^+]/[MH^+]$ were securely determined through analyses of more than 9000 spectra.

The log–log plot of $[AH^+]/[MH^+]$ against the mixing ratio $([A]/[M])^0$ revealed a peculiar characteristic (plateau–linear increase–plateau) as $([A]/[M])^0$ increases for CHCA; plateau regions were not observed for DHB. The linear increase was interpreted in terms of AH^+ formation by the proton-transfer reaction $MH^+ + A \rightleftharpoons M + AH^+$, which reached thermal equilibrium in the MALDI plume.

The A/M mixing ratios $([A]/[M])^0_e$ at which $[AH^+]/[MH^+] = 1$ was observed, determined from each log–log plot for the 20 amino acids, were plotted with respect to the GB. Clear correlations between $([A]/[M])^0_e$ and GB were seen in the plots using both CHCA and DHB, except for basic amino acids, and were well analyzed by the above proton-transfer model. The GB values and equilibrium temperatures for CHCA and DHB were determined to be 851 kJ mol^{-1} and 1510 K and 830 kJ mol^{-1} and 1330 K, respectively, and agreed with values in the literature.[8,16–18] These results validate the present thermochemical interpretation of protonation efficiency for amino acids of the present study.

The protonation efficiencies for basic amino acids Lys, His, and Arg reveal lower $([A]/[M])^0_e$ values than those expected from the GB by a factor of 10^{-1}–10^{-2}. The deviations were explained by considering the conformer-dependent effective GB; the GB of basic amino acids is related to the proton affinity of side chains, while the proton acceptor role of the side chain is assumed to be blocked by an intramolecular hydrogen bond arising from the presence of a zwitterionic form in the MALDI plume.

References

1 R. J. Cotter, *Time-of-flight Mass Spectrometry: Instrumentation and Applications in Biological Research*, American Chemical Society, Washington, DC, **1997**.

2 G. Siuzdak, *The Expanding Role of Mass Spectrometry in Biotechnology*, MCC Press, San Diego, **2003**.

3 F. Hillenkamp, M. Karas, in *MALDI MS*, ed. by F. Hillenkamp, J. P-Katalinić, WILEY-VCH, Weinheim, **2007**.

4 R. Knochenmuss, *Analyst* **2006**, *131*, 966.

5 B. H. Wang, K. Dreisewerd, U. Bahr, M. Karas, F. Hillenkamp, *J. Am. Soc. Mass Spectrom.* **1993**, *4*, 393.

6 P.-C. Liao, J. Allison, *J. Mass Spectrom.* **1995**, *30*, 408.

7 A. G. Harrison, *Chemical Ionization Mass Spectrometry*, CRC Press, Boca Raton, **1992**.

8 G. R. Kinsel, D. Yao, F. H. Yassin, D. S. Marynick, *Eur. J. Mass Spectrom.* **2006**, *12*, 359.

9 T. Nishikaze, M. Takayama, *Rapid Commun. Mass Spectrom.* **2006**, *20*, 376.

10 M. Karas, U. Bahr, U. Gießmann, *Mass Spectrom. Rev.* **1991**, *10*, 335.

11 A. A. Puretzky, D. B. Geohegan, G. B. Hurst, M. V. Buchanan, B. S. Luk'yanchuk, *Phys. Rev. Lett.* **1999**, *83*, 444.

12 C. D. Mowry, M. V. Johnston, *Rapid Commun. Mass Spectrom.* **1993**, *7*, 569.

13 R. Knochenmuss, V. Karbach, U. Wiesli, K. Breuker, R. Zenobi, *Rapid Commun. Mass Spectrom.* **1998**, *12*, 529.

14 R. Knochenmuss, R. Zenobi, *Chem. Rev.* **2003**, *103*, 441.

15 A. G. Harrison, *Mass Spectrom. Rev.* **1997**, *16*, 201.

16 R. J. J. M. Steenvoorden, K. Breuker, R. Zenobi, *Eur. J. Mass Spectrom.* **1997**, *3*, 339.

17 M. Mormann, S. Bashir, P. J. Derrick, D. Kuck, *J. Am. Soc. Mass Spectrom.* **2000**, *11*, 544.

18 F. H. Yassin, D. S. Marynick, *Mol. Phys.* **2005**, *103*, 183.

19 E. Stevenson, K. Breuker, R. Zenobi, *J. Mass Spectrom.* **2000**, *35*, 1035.

20 A. Koubenakis, V. Frankevich, J. Zhang, R. Zenobi, *J. Phys. Chem. A* **2004**, *108*, 2405.

21 J. H. Jensen, M. S. Gordon, *J. Am. Chem. Soc.* **1991**, *113*, 7917.

22 J. Rak, P. Skurski, J. Simons, M. Gutowski, *J. Am. Chem. Soc.* **2001**, *123*, 11695.